Exploring the Potential of Water Soluble Cu(II) Complexes with MPA-CdTe Quantum Dots for Photoinduced Electron Transfer

Niharika Krishna Botcha[1], Rithvik R. Gutha[2], Seyed M. Sadeghi[2], Anusree Mukherjee[3*]

[1]Department of Chemistry, The University of Alabama in Huntsville, 301 Sparkman Drive, Huntsville, AL 35899, USA

[2]Department of Physics and Astronomy, The University of Alabama in Huntsville, 301 Sparkman Drive, Huntsville, AL 35899, USA

[3]Department of Chemistry and Geosciences, Jacksonville State University, 700 Pelham Rd N, Jacksonville, AL 36265, USA

*Correspondence: amukherjee@jsu.edu

Ligand Synthesis

The ligands for complexes **1-3** (BPMEN, 345BPMEN and PDP respectively) were synthesized following the procedures listed in literature.[1,2]

Caution! Although no problems occurred in this work, perchlorate salts mixed with organic compounds can be explosive. All necessary safety precautions should be followed.

Synthesis of [CuBPMEN]$(ClO_4)_2$ (1)

The complex **1** was prepared by following a similar procedure as reported in literature.[1–4] The ligand BPMEN (0.271 g, 1 mmol) dissolved in methanol (4 mL) was added dropwise to a stirring solution of $Cu(ClO_4)_2 \cdot 6H_2O$ (0.371 g, 1 mmol) in methanol (4 mL). A dark blue solution was obtained upon addition. Evaporation of the solvent gave a dark blue colored powder (0.525 g, Yield: 98 %).

ESI-MS (in CH_3OH) for $[(CuBPMEN)ClO_4]^+$ (z = 1) m/z 432.12 (experimental) m/z 432.10 (theoretical) and for $[(CuBPMEN)]^{2+}$ (z = 2) m/z 166.59 (experimental) m/z 166.56 (theoretical). Elemental analysis Calculated (%): C 36.07, H 4.16, N 10.52 Found (%): C 36.89, H 4.92, N 9.62. UV–Vis (λ_{max} (nm)) [ε (M^{-1} cm^{-1})] in H_2O at 25 °C: 631 (140).

Synthesis of $[Cu345BPMEN](ClO_4)_2$ (2)

The complex **2** was prepared by following similar procedure as reported for **1**. The ligand 345BPMEN (0.102 g, 0.512 mmol) dissolved in methanol (4 mL) was added dropwise to a stirring solution of $Cu(ClO_4)_2 \cdot 6H_2O$ (0.190 g, 0.512 mmol) in methanol (4 mL). A blue solution was obtained upon addition. Evaporation of the solvent gave a blue colored powder (0.590 g, Yield: 91 %).

ESI-MS (in CH_3OH) for $[(Cu345BPMEN)ClO_4]^+$ (z = 1) m/z 548.22 (experimental) m/z 548.31 (theoretical) and for $[(Cu345BPMEN)]^{2+}$ (z = 2) m/z 224.73 (experimental) m/z 224.85 (theoretical). Elemental analysis Calculated (%): C 38.53, H 5.90, N 7.81 Found (%): C 38.29, H 5.50, N 8.29. UV–Vis (λ_{max} (nm)) [ε (M^{-1} cm^{-1})] in H_2O at 25 °C: 630 (128).

Synthesis of $[CuPDP](ClO_4)_2$ (3)

The complex **3** was prepared by following similar procedure as reported for **1**. The ligand PDP (0.150 g, 0.465 mmol) dissolved in methanol (3 mL) was added dropwise to a stirring solution of $Cu(ClO_4)_2 \cdot 6H_2O$ (0.173 g, 0.465 mmol) in methanol (3 mL). A violet solution was obtained upon addition. Evaporation of the solvent gave a violet blue colored powder (0.254 g, Yield: 93 %). ESI-MS (in CH_3OH) for $[(CuPDP)ClO_4]^+$ (z = 1) m/z 484.16 (experimental) m/z 484.15 (theoretical) and for $[(CuPDP)]^{2+}$ (z = 2) m/z 192.66 (experimental) m/z 192.67 (theoretical). Elemental analysis Calculated (%): C 39.84, H 4.68, N 9.37, Cl 11.70 Found (%): C 39.96, H 4.52, N 9.37, Cl 11.70. UV–Vis (λ_{max} (nm)) [ε (M^{-1} cm^{-1})] in H_2O at 25 °C: 593 (95).

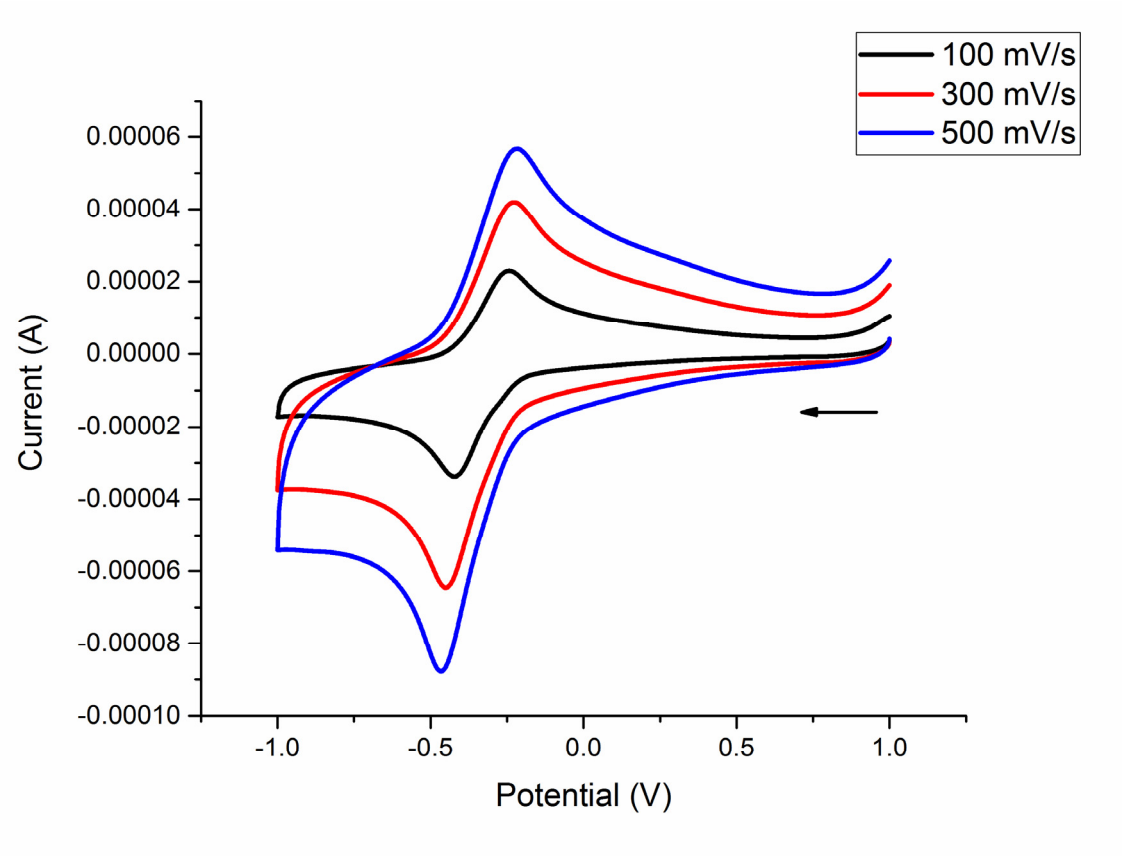

Figure S1: Cyclic Voltammogram of **1** in water under N_2 with Ag/AgCl as the reference electrode and 0.1 M KCl as the supporting electrolyte

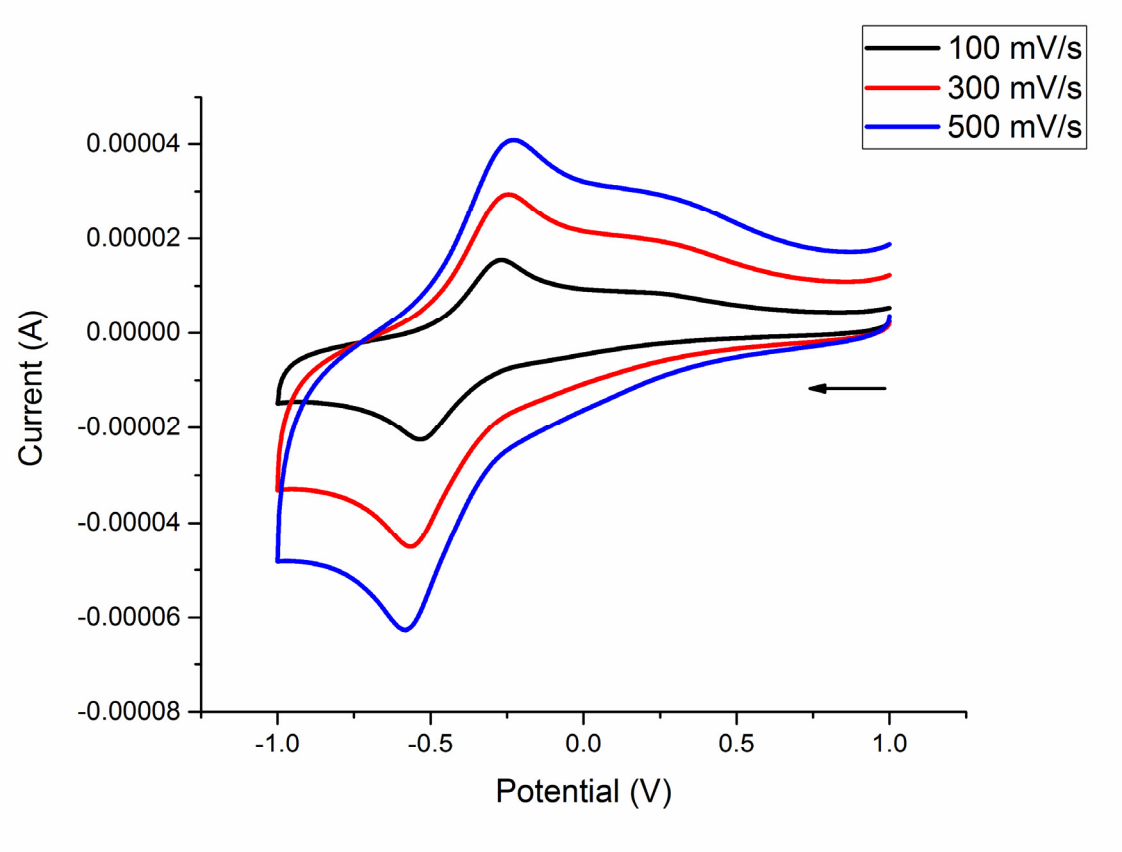

Figure S2: Cyclic Voltammogram of **2** in water under N_2 with Ag/AgCl as the reference electrode and 0.1 M KCl as the supporting electrolyte

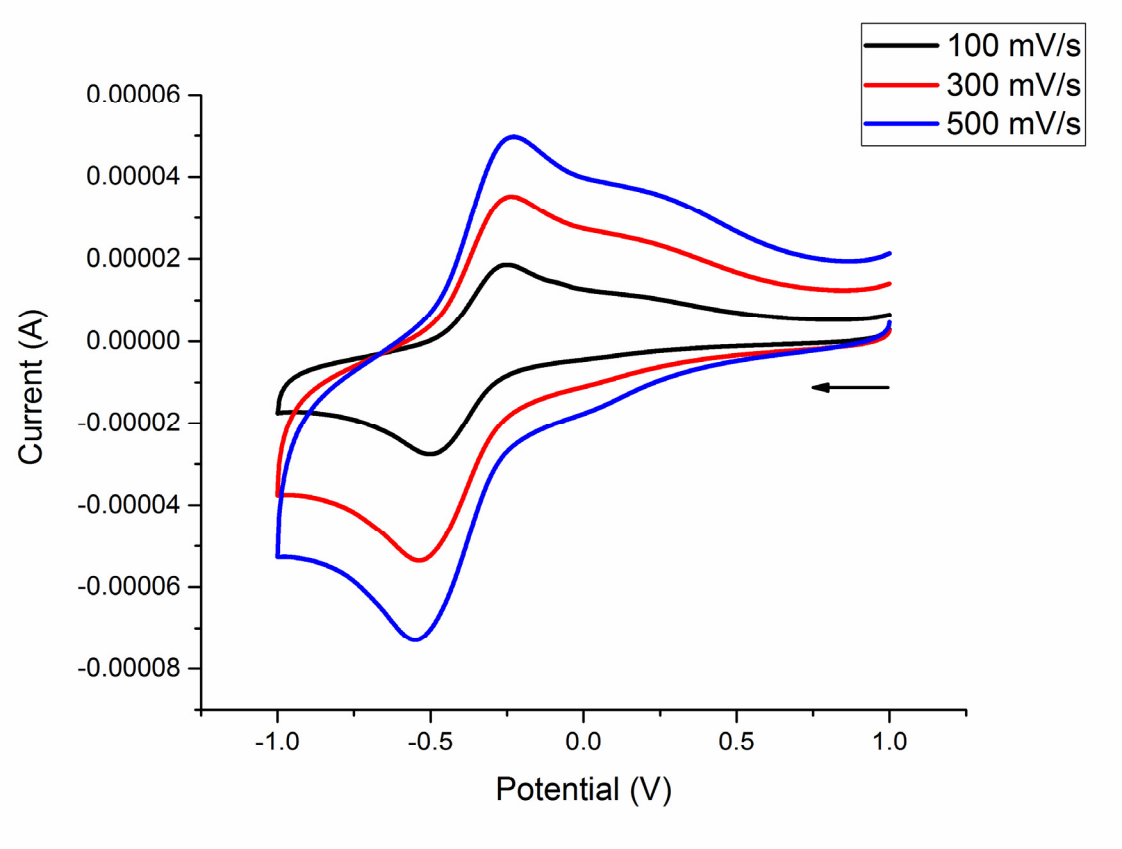

Figure S3: Cyclic Voltammogram of **3** in water under N_2 with Ag/AgCl as the reference electrode and 0.1 M KCl as the supporting electrolyte

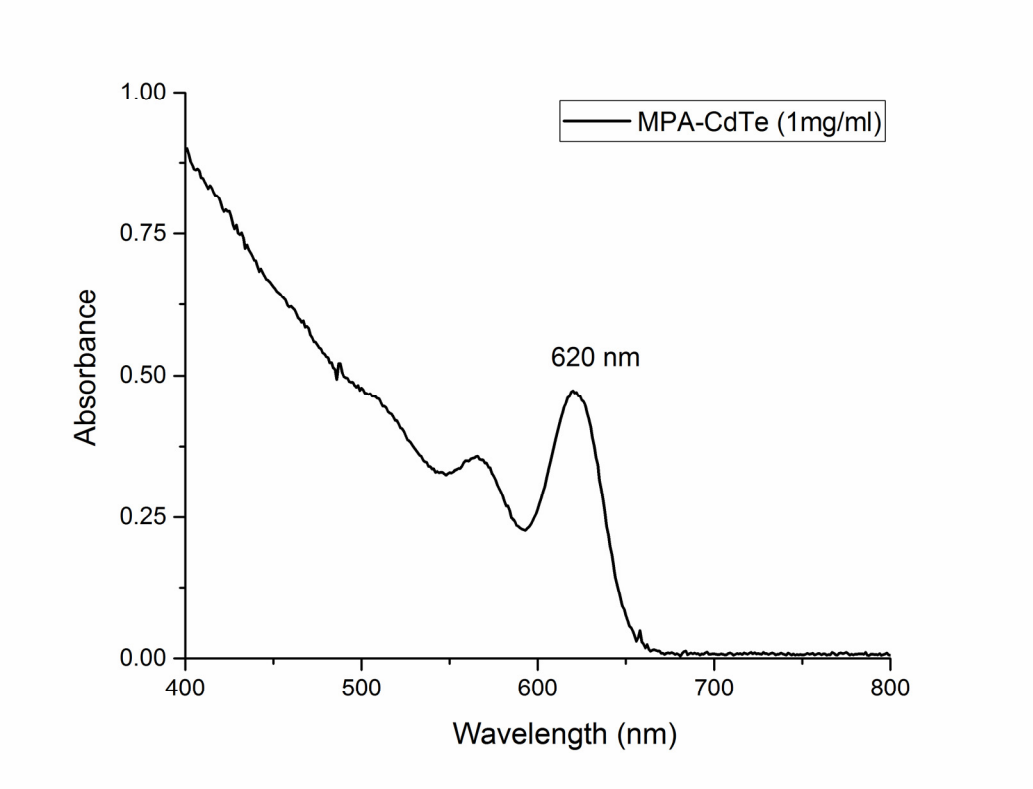

Figure S4: UV-Vis absorption spectra of MPA-CdTe QDs (2.8×10^{-6} M, 1 mg/mL)

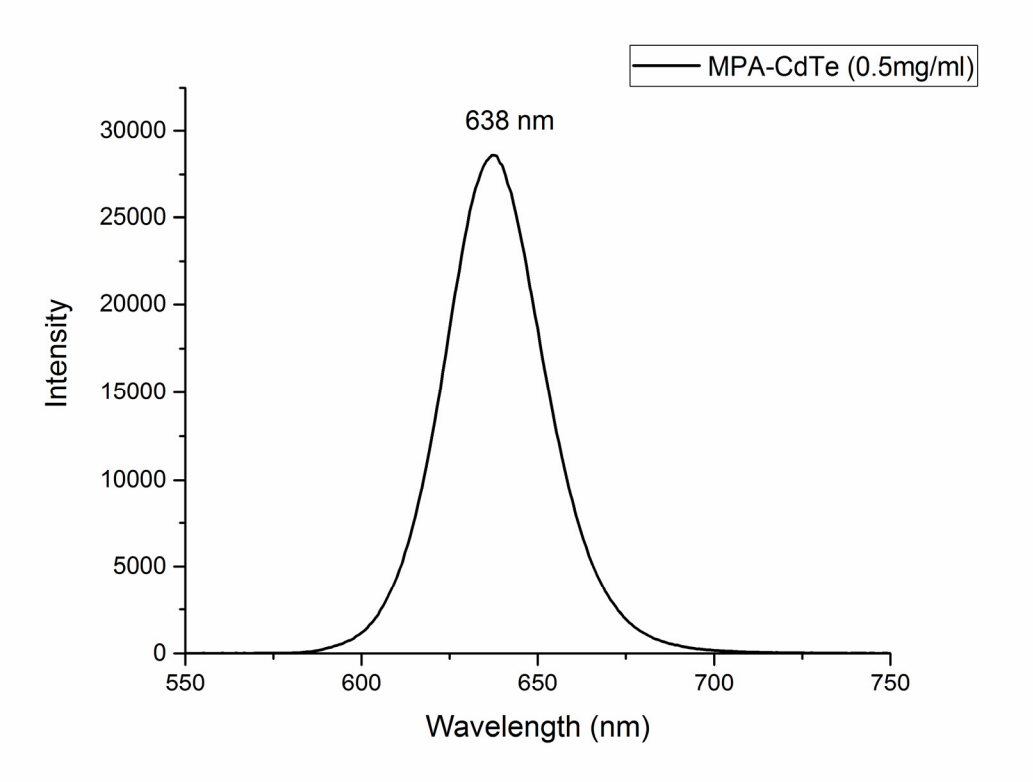

Figure S5: Emission spectra of MPA-CdTe QDs (1.4×10^{-6} M, 0.5 mg/mL)

The concentration of the MPA-CdTe QDs was determined as 2.8×10^{-6} M (1 mg/mL) using the Beer–Lambert law (Figure S4). On the basis of the absorption band centered at 620 nm, the particle size of the MPA-CdTe QDs was determined to be 3.9 nm using the equations S1-S2.[5]

$$D = (9.8127 \times 10^{-7})\lambda^3 - (1.7147 \times 10^{-3})\lambda^2 + 1.0064\lambda - 194.84 \quad (S1)$$

$$\varepsilon = 10043(D)^{2.12} \quad (S2)$$

wherein D (nm) is the diameter or size of a given nanocrystals sample, λ is the wavelength of the first absorption peak (from low energy) of the corresponding sample and ε is the extinction coefficient of the corresponding sample.

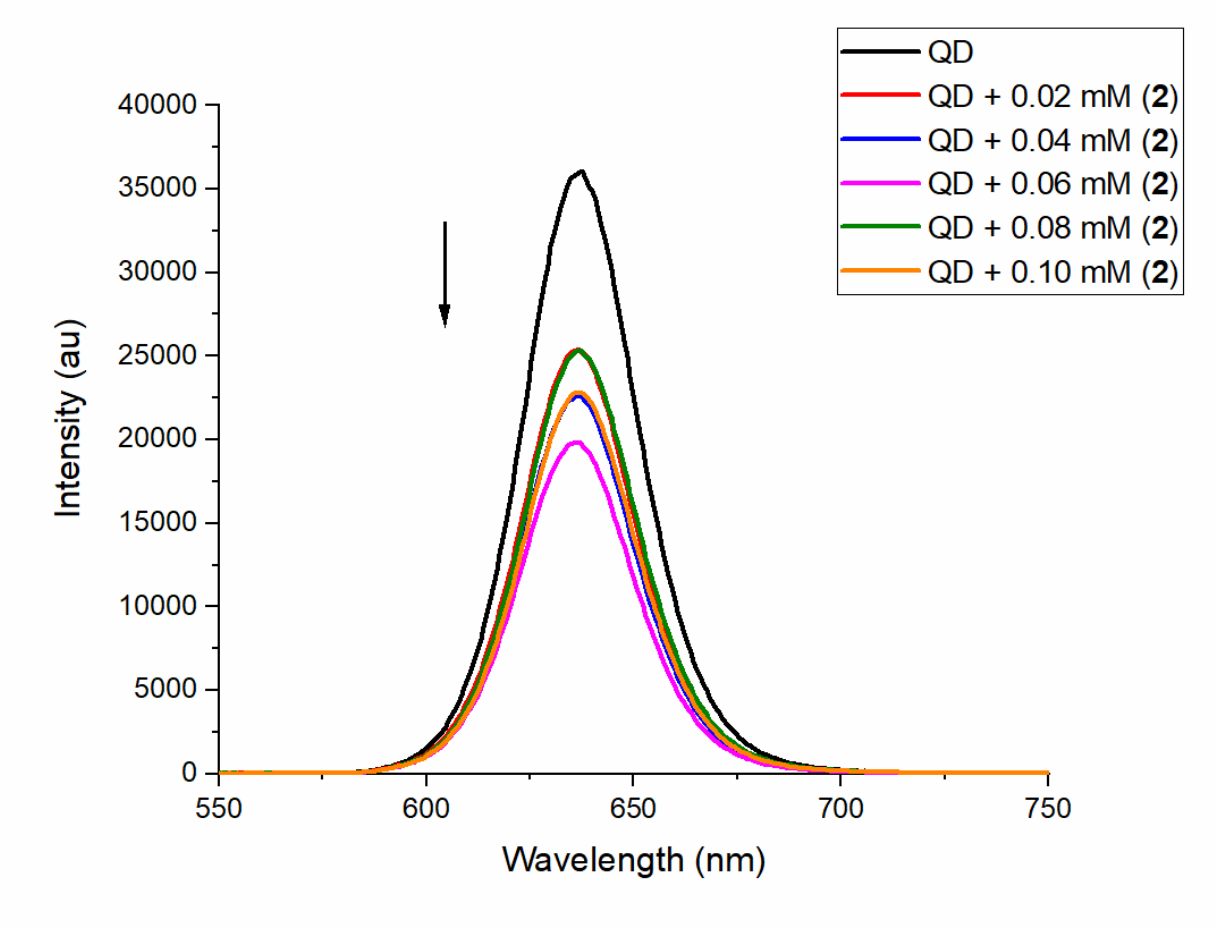

Figure S6: Emission spectra of MPA-CdTe quantum dots (1.4×10^{-6} M, 0.5 mg/mL) with increasing concentration of **2** (0 to 0.10 $\times10^{-3}$ M) in water (excitation wavelength: 514 nm)

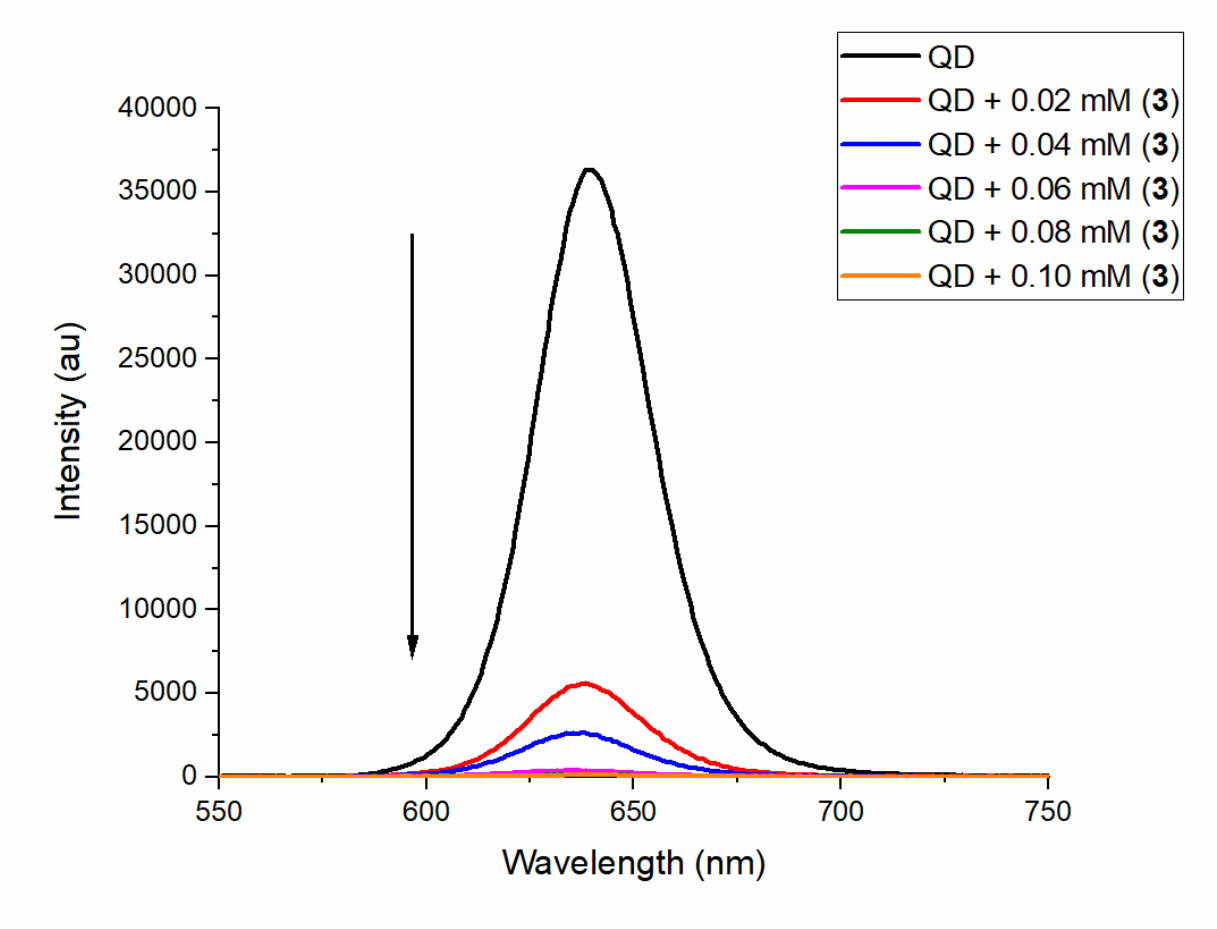

Figure S7: Emission spectra of MPA-CdTe quantum dots (1.4×10^{-6} M, 0.5 mg/mL) with increasing concentration of **3** (0 to 0.10 $\times10^{-3}$ M) in water (excitation wavelength: 514 nm)

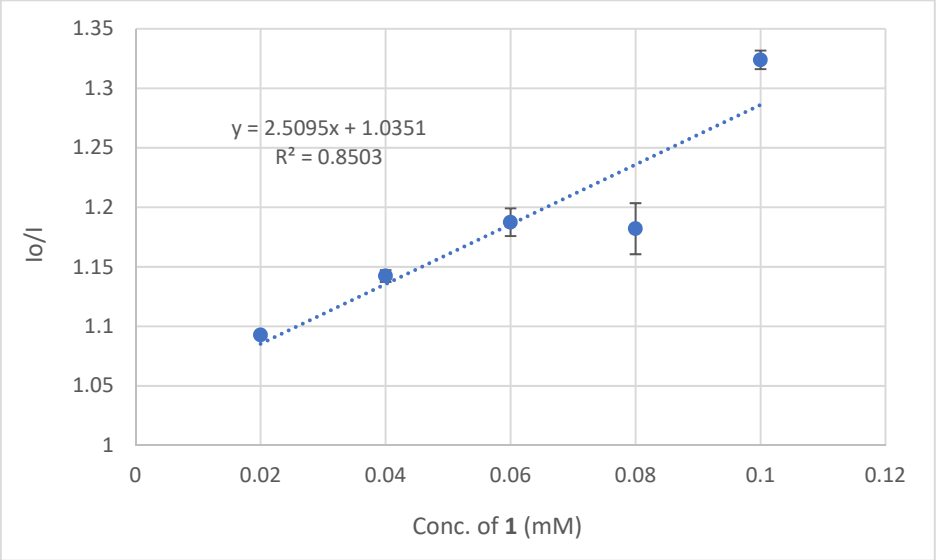

Figure S8: Stern-Volmer plot for the luminescence quenching of MPA-CdTe QDs with **1**

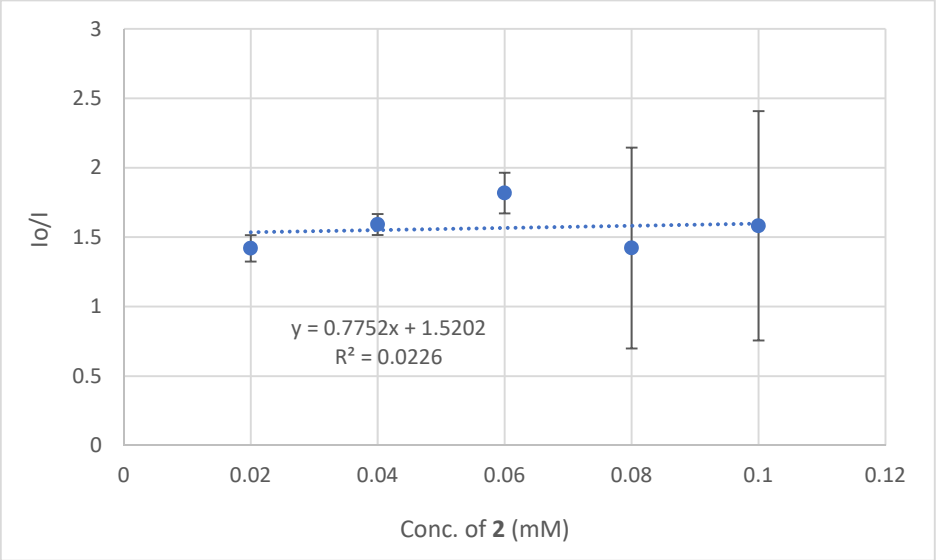

Figure S9: Stern-Volmer plot for the luminescence quenching of MPA-CdTe QDs with **2**

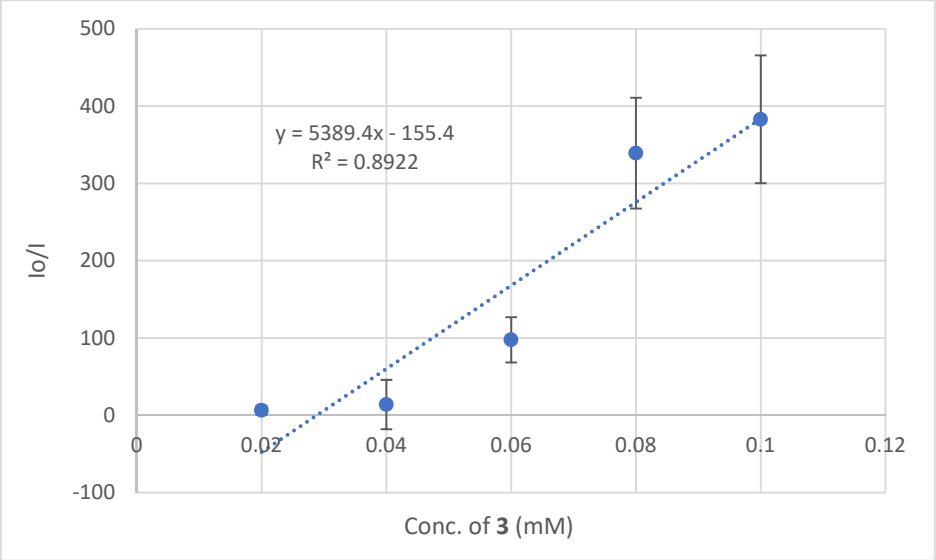

Figure S10: Stern-Volmer plot for the luminescence quenching of MPA-CdTe QDs with **3**

Table S1: The Stern–Volmer quenching constant K_{sv} for the complexes **1** and **3**

Complex	K_{sv} (M^{-1})
1	3.0×10^3
3	3.3×10^6

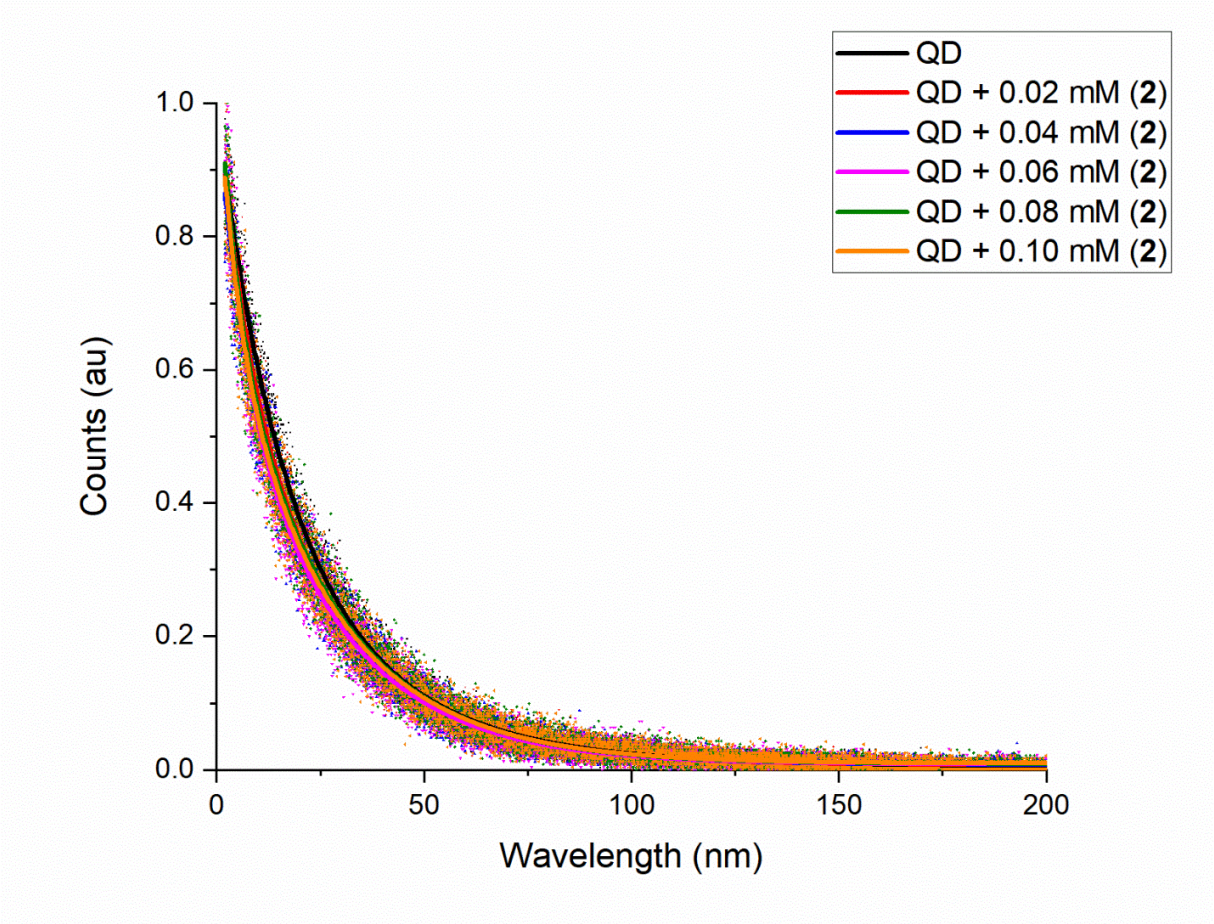

Figure S11: The lifetime of MPA-CdTe quantum dots (1.4×10^{-6} M, 0.5 mg/mL) with increasing concentrations of **2** (0 to 0.10 $\times10^{-3}$ M) in water (excitation wavelength: 450 nm).

The decay lifetime was best fit by a biexponential function (Equation S3).

$$A_1\exp(t/\tau_1) + A_2\exp(t/\tau_2) \qquad \text{(S3)}$$

Where, A_1 and A_2 are the amplitudes and τ_1 and τ_2 are the lifetimes.

Table S2: Mean lifetimes of the quantum dots in the presence of complexes **1-2**

	Mean Lifetime for **1** (ns)	Mean Lifetime for **2** (ns)
QD	25	25
QD + 0.02 mM	24	24
QD + 0.04 mM	24	24
QD + 0.06 mM	25	24
QD + 0.08 mM	24	24
QD + 0.10 mM	25	24

Table S3: Biexponential fit parameters and mean lifetimes for **1**

	A_1	τ_1 (ns)	A_2	τ_2 (ns)	Average τ (ns)
QD	0.55	15.57	0.30	33.46	25.3
QD + 0.02 mM (**1**)	0.37	12.73	0.46	28.56	24.3
QD + 0.04 mM (**1**)	0.25	9.99	0.56	26.49	24.1
QD + 0.06 mM (**1**)	0.37	11.69	0.50	28.47	24.5
QD + 0.08 mM (**1**)	0.21	7.83	0.63	25.60	23.9
QD + 0.10 mM (**1**)	0.28	9.18	0.55	27.28	24.6

Table S4: Biexponential fit parameters and mean lifetimes for **2**

	A_1	τ_1 (ns)	A_2	τ_2 (ns)	Average τ (ns)
QD	0.51	15.01	0.38	31.72	25.2
QD + 0.02 mM (**2**)	0.21	7.03	0.63	25.46	23.8
QD + 0.04 mM (**2**)	0.18	6.08	0.62	25.11	23.8
QD + 0.06 mM (**2**)	0.27	5.07	0.62	25.11	23.5
QD + 0.08 mM (**2**)	0.18	4.61	0.65	25.10	24.1
QD + 0.10 mM (**2**)	0.24	4.80	0.65	25.44	24.1

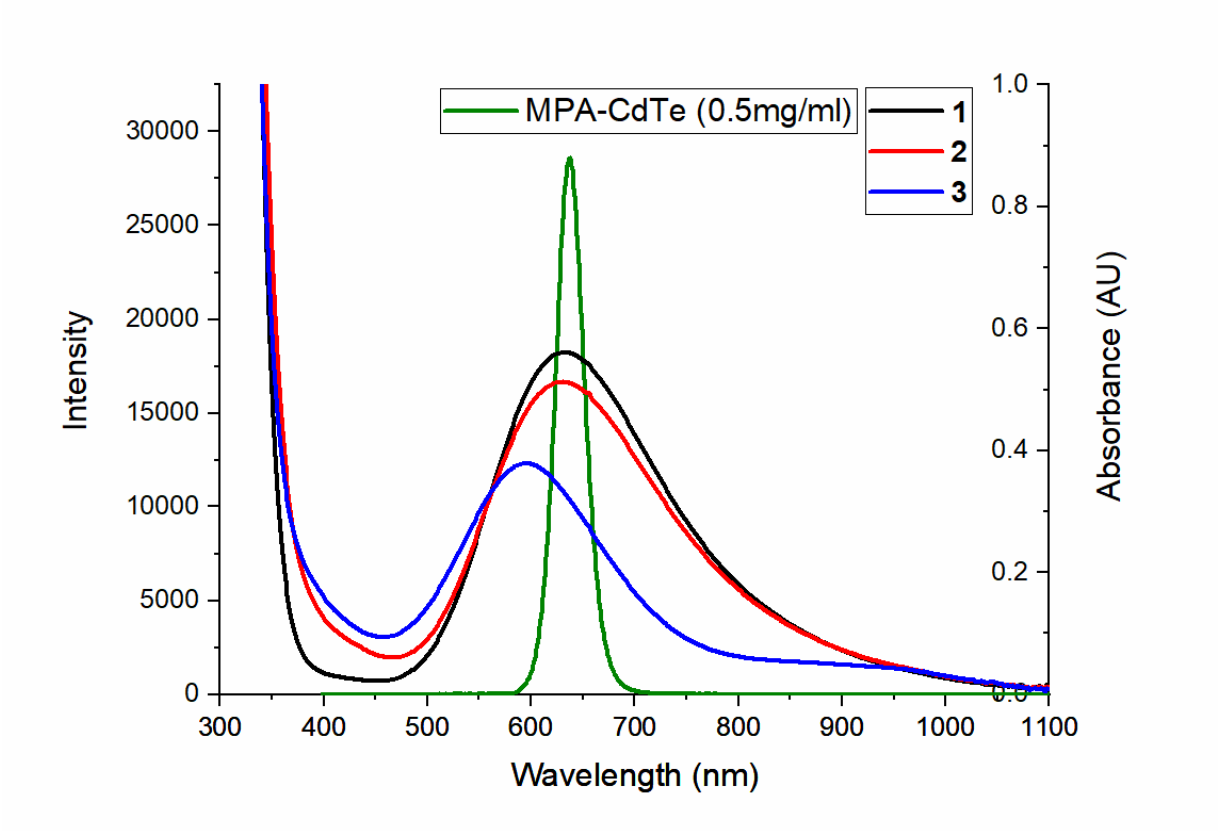

Figure S12: Overlay of the absorption maxima of the complexes **1-3** (scale on right) and the emission maximum of the MPA-CdTe QDs (scale on left).

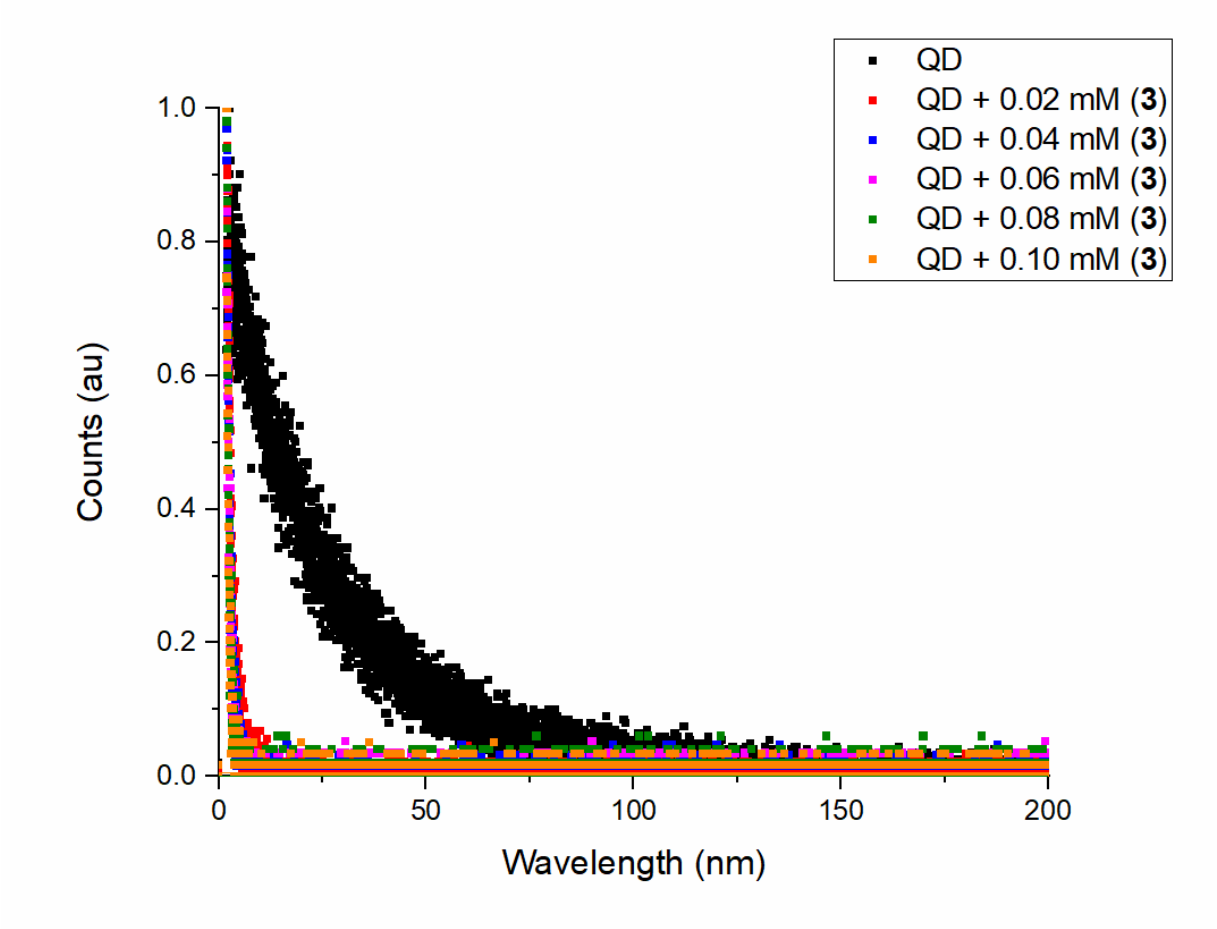

Figure S13: The lifetime of MPA-CdTe quantum dots (1.4×10^{-6} M, 0.5 mg/mL) with increasing concentrations of **3** (0 to 0.10 $\times10^{-3}$ M) in water (excitation wavelength: 450 nm)

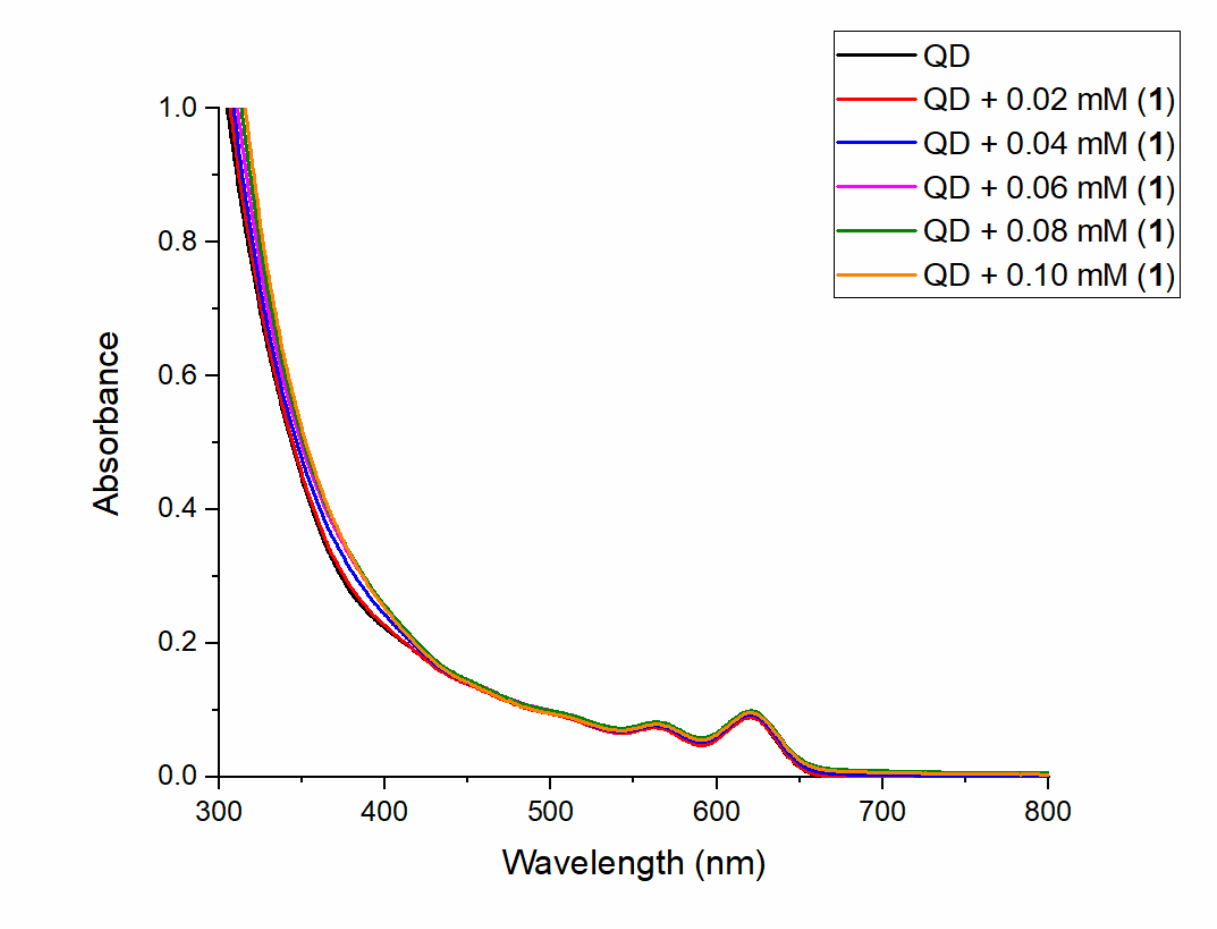

Figure S14: UV-Vis absorption spectra of MPA-CdTe quantum dots (1.4×10^{-6} M, 0.5 mg/mL) with increasing concentration of **1** (0 to 0.10×10^{-3} M) in water

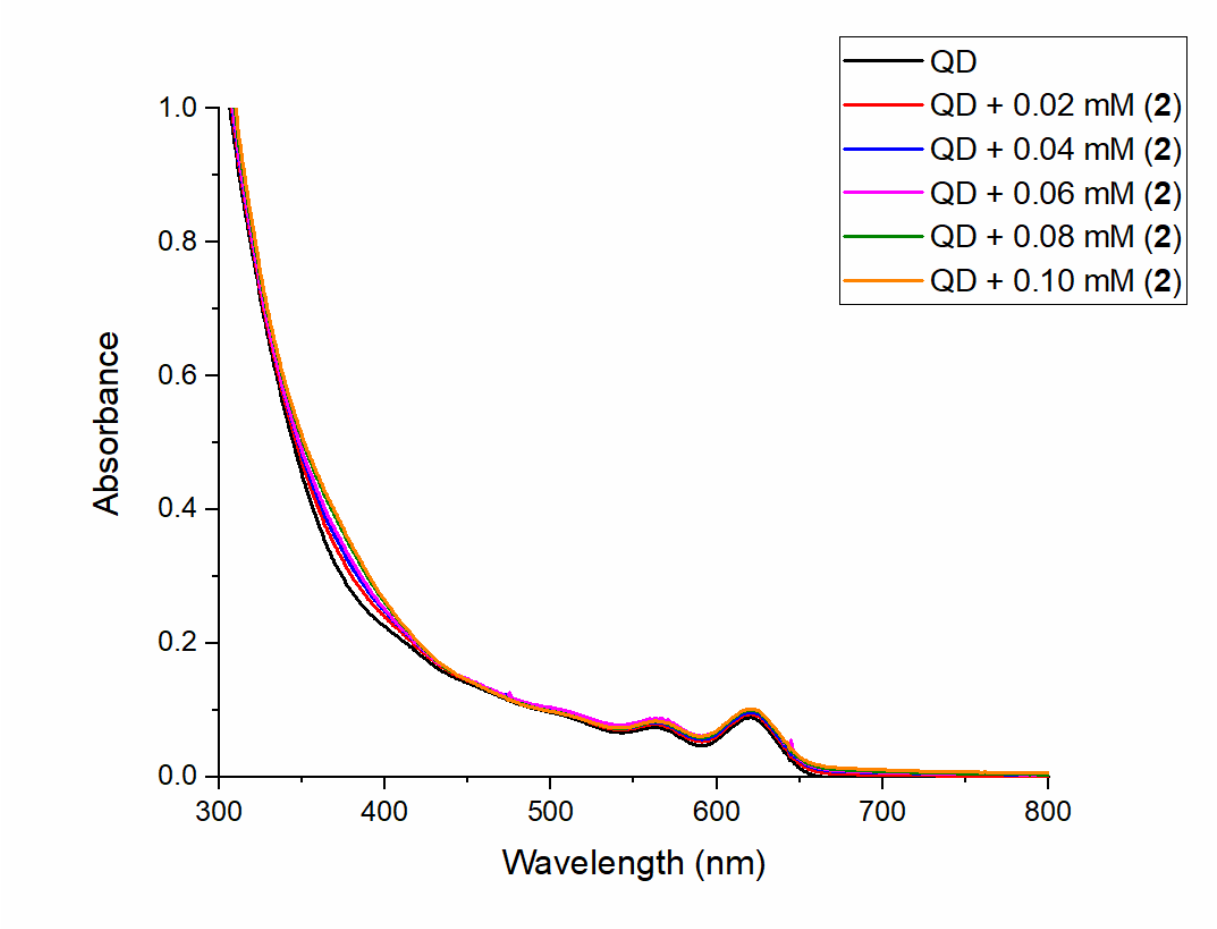

Figure S15: UV-Vis absorption spectra of MPA-CdTe quantum dots (1.4×10^{-6} M, 0.5 mg/mL) with increasing concentration of **2** (0 to 0.10 $\times10^{-3}$ M) in water

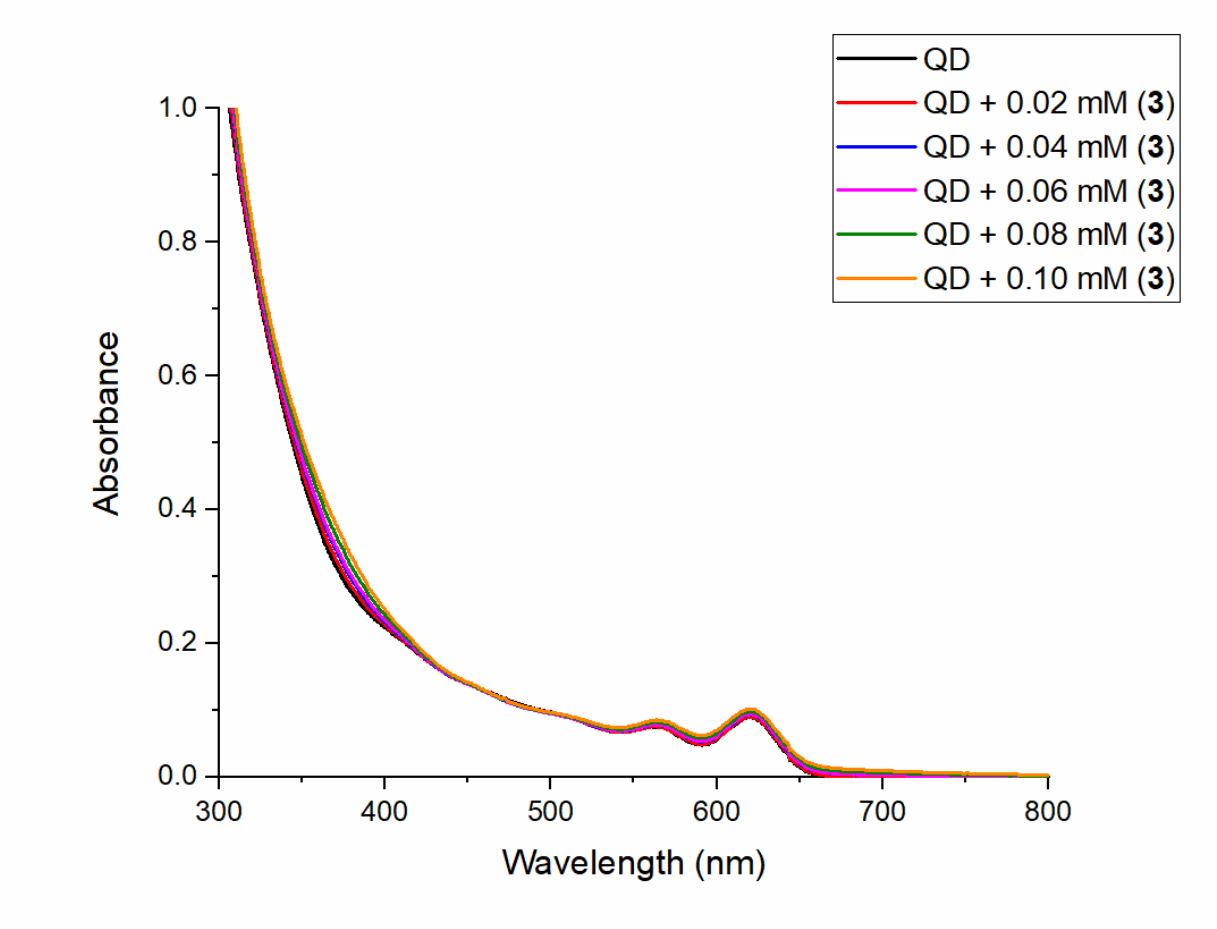

Figure S16: UV-Vis absorption spectra of MPA-CdTe quantum dots (1.4×10^{-6} M, 0.5 mg/mL) with increasing concentration of **3** (0 to 0.10×10^{-3} M) in water

Table S5: Hydrodynamic sizes for QDs and complexes **1-3** from DLS measurements

Complex	QD + 0.10 mM (Complex) nm	QD + 0.20 mM (Complex) nm	QD + 0.30 mM (Complex) nm	QD + 0.40 mM (Complex) nm
1	N/R	129.2	351.9	2585
		142	893.1	3071
		221.3	1222	3679
2	N/R	N/R	464.9	463.8
			406.1	374
			549.2	541.4
3	N/R	N/R	201.1	672.2
			525.5	421.5
			410	382.4

N/R: No measurement could be recorded

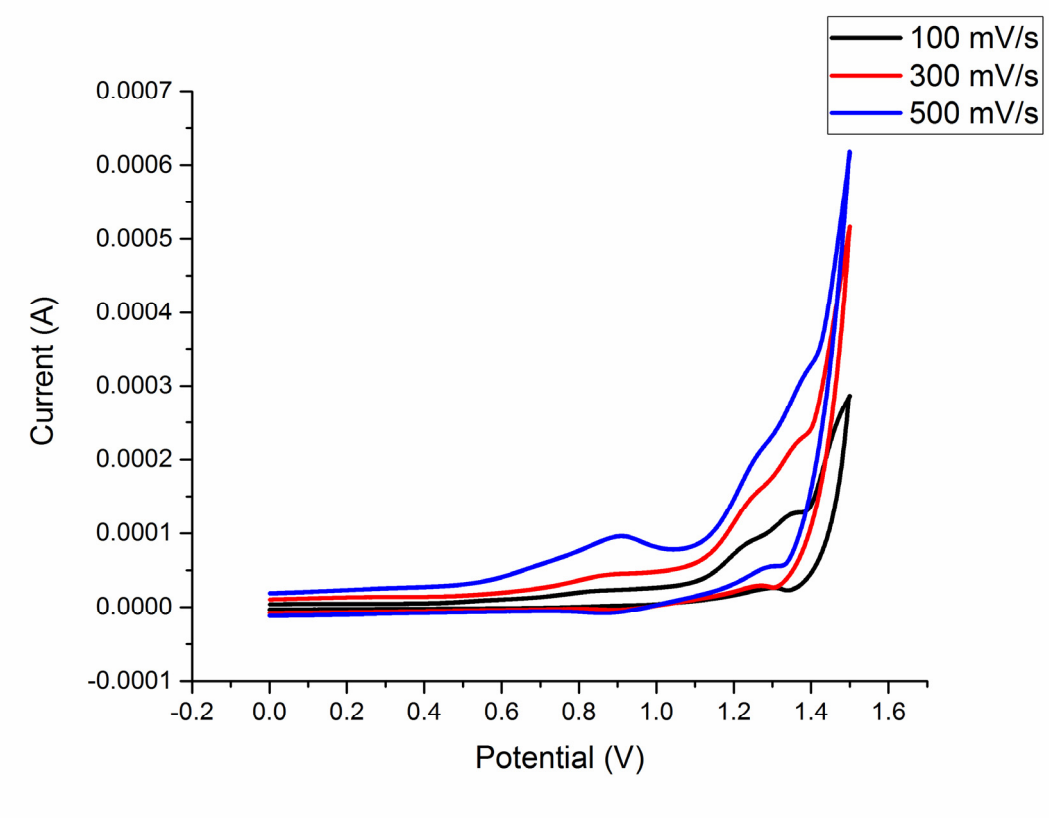

Figure S17: Cyclic Voltammogram of MPA-CdTe QDs in water under N_2 with Ag/AgCl as the reference electrode and 0.1 M KCl as the supporting electrolyte

The bandgap (E_g) calculated from the absorption spectra of the MPA-CdTe QDs is 2 eV (Figure S4). The anodic peak potential of the MPA-CdTe QDs (Figure S14) is +0.907 V vs Ag/AgCl, which gives an estimated value for the valence band energy level (E_{vb}) as +1.2 V vs NHE. Utilizing the values for E_{vb} and E_g, the calculated value for the conduction band energy level (E_{cb}) for the MPA-CdTe QDs is -0.8 V vs NHE.

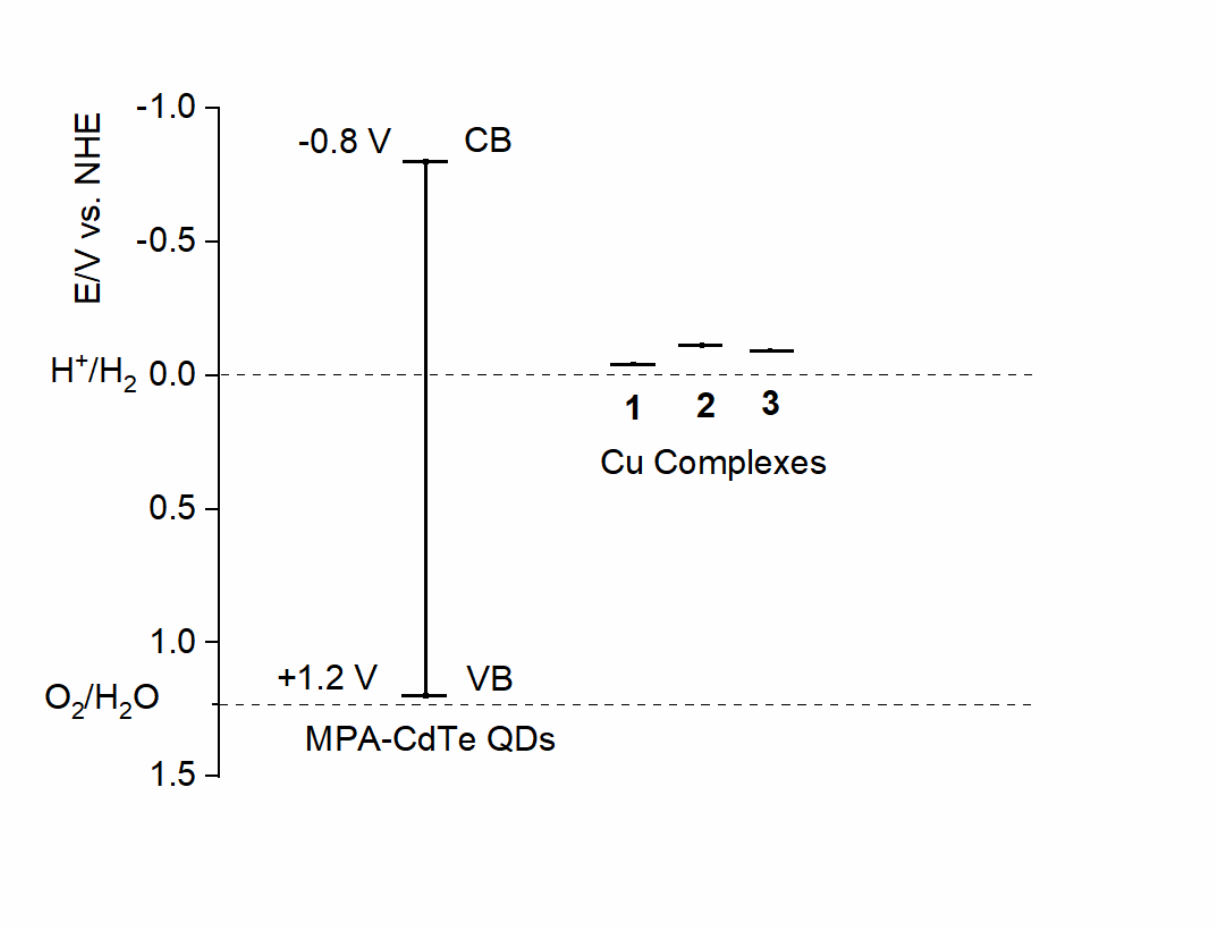

Figure S18: Bandgap (vs. NHE) of the MPA-CdTe quantum dots and the reduction potentials (vs. NHE) of the complexes **1–3**

References

(1) Botcha, N. K. Chemical Oxidation and Photoinduced Electron Transfer by Nickel and Copper Complexes : A Dissertation, The University of Alabama in Huntsville, Huntsville, 2021.
(2) Botcha, N. K.; Gutha, R. R.; Sadeghi, S. M.; Mukherjee, A. Synthesis of Water-Soluble Ni(II) Complexes and Their Role in Photo-Induced Electron Transfer with MPA-CdTe Quantum Dots. *Photosynth Res* **2019**. https://doi.org/10.1007/s11120-019-00668-z.
(3) Khazanov, T. M.; Botcha, N. K.; Yergeshbayeva, S.; Shatruk, M.; Mukherjee, A. Investigating Reactivity and Electronic Structure of Copper(II)-Polypyridyl Complexes

and Hydrogen Peroxide. *Inorganica Chimica Acta* **2021**, *516*, 120168. https://doi.org/10.1016/j.ica.2020.120168.
(4) Singh, N.; Botcha, N. K.; Jones, T. M.; Ertem, M. Z.; Niklas, J.; Farquhar, E. R.; Poluektov, O. G.; Mukherjee, A. Reactivity of Bio-Inspired Cu(II) (N2/Py2) Complexes with Peroxide at Room Temperature. *Journal of Inorganic Biochemistry* **2019**, *197*, 110674. https://doi.org/10.1016/j.jinorgbio.2019.03.014.
(5) Yu, W. W.; Qu, L.; Guo, W.; Peng, X. Experimental Determination of the Extinction Coefficient of CdTe, CdSe, and CdS Nanocrystals. *Chem. Mater.* **2003**, *15* (14), 2854–2860. https://doi.org/10.1021/cm034081k.